

Plate velocities in the hotspot reference frame

W. Jason Morgan

*Department of Earth and Planetary Sciences, Harvard University, Cambridge, Massachusetts
02138, USA*

Jason Phipps Morgan

*Department of Earth and Atmospheric Sciences, Cornell University, Ithaca, New York 14853,
USA*

ABSTRACT

We present a table of 57 hotspots distributed on all major plates with a short discussion of the 'present-day' (average over most recent ~ 5 Ma) direction and velocity for each hotspot track, with estimated errors. An electronic supplement has a discussion of each track and references to the data sources. Using the entries in Table 1, we found Pacific plate motion is a rotation about a pole at 59.33°N , 85.10°W with a rate that gives a velocity at the pole's 'equator' of 89.20 mm/yr ($= -0.8029$ $^\circ/\text{Ma}$). The errors in this pole/rate are of the order $\pm 2^\circ\text{N}$, $\pm 4^\circ\text{W}$, ± 3 mm/yr. The motions of other plates are then determined by NUVEL-1A.

The large number of close, many very short, tracks in the Pacific superswell region precludes all hotspots being rooted near the core-mantle boundary. In general, we think asthenosphere is hotter than mantle just below it (in a potential temperature sense). Asthenosphere is very hot – brought up from the core-mantle boundary by plumes. Mantle is cooled by downgoing slabs, and a convective stability is established whereby mantle rises only at plumes and sinks only at trenches. We propose that this normal mantle geotherm is overwhelmed by much-larger-than-average mantle upwelling in superswell areas, making many short-lived instabilities in the upper mantle. Because soft asthenosphere so decouples plates from mantle below, instabilities in the

upper mantle (perhaps even above the 660-km discontinuity) are relatively 'fixed' in comparison to plate motions. With the mantle velocity contribution being minor, tracks are parallel to and have rates set by plate velocities.

INTRODUCTION

The bulk of this paper is an electronic supplement which gives the supporting data for each entry in Table 1 (this paper). This table is the main difference between this work and previous papers solving for present-day plate motions in a hotspot reference frame. In a future paper, we shall describe in detail the algorithm we applied to the data to solve for the best velocity model, here we briefly describe the algorithm and go directly to our main findings. One of the novel features of our method is the use of 'azimuth only' data when solving for the optimum plate velocity solution – the relative velocities between the plates supplies the velocity information needed and the greater errors in track rates do not contaminate the more accurately determined track-azimuth data. An azimuth-only technique was recently incorporated in the latest paper by Gripp and Gordon (2002) – what distinguishes our work from theirs is our much larger, more globally distributed data set. Note, in their final ('best') solution, Gripp and Gordon (2002) include with their azimuth-only data the rate data from two tracks: Hawaii and Society. We think both of these tracks have rates biased 'high' – these rates were determined with (early, some of the very first) K-Ar measurements, not the more accurate $^{40}\text{Ar}/^{39}\text{Ar}$ measurements. Their 'final' numbers thus give a velocity of the Pacific plate that is too high, and consequently their fit of tracks in European, African, and Indian regions is worse than their earlier models. (Keep their pole the same and slow down the Pacific, and their fit to tracks in these far away regions would become very good.)

Table 1 summarizes all the discussion that follows in this paper. It gives the latitude and longitude of each hotspot and the plate it is on, a 'weight' (which will be defined in the next paragraph), the observed azimuth of its (present-day) track and an estimated error of this

azimuth, where possible the measured velocity (with estimated error), and in the final columns the azimuth and rate predicted by our model. We tried to determine the azimuth over as short an interval as possible, usually over a 5 Ma interval on fast-moving plates (Pacific, Nazca) and over 10 Ma on slower plates. If the interval is longer, it is noted in the discussion of the track in the electronic supplement. We give a model azimuth and rate even for places where we cannot measure an azimuth (for example, at the questionable Kilimanjaro) – these places are 'interesting' and knowing a direction predicted by consistency on the same plate could aid in recognizing a pattern (*e.g.*, if Etna had a track, where would you most likely find it?). We have not considered how 'deep' the source of a hotspot is located (we think there are too many in the list and several that are too close to one another for all of them to have deep origins). A finite-motion reconstruction of long-lived tracks would be needed to test the permanence of a source – this list was only used to test the 'instantaneous' present-day motions. However the results we obtain with our model show the hotspots in this list provide a very useful reference frame for present-day motions of plates over something 'fixed' to the mantle. We think the asthenosphere almost completely decouples the plates from a much more fixed mantle below the asthenosphere, and even minor hotspots that may not originate at the core-mantle boundary appear to have negligible motion with respect to this general frame in our 'instantaneous' inversion.

The weight 'w' is a number between 1 and 0.2; it is our estimate of the accuracy of the azimuth of the track of a hotspot. The weight is based on the estimated error of the azimuth of the track (σ_{azim}), with downward adjustment of the weight at some tracks based on qualitative criteria as discussed in the electronic supplement. The general rule for assigning weights is: ($\sigma_{\text{azim}} \leq 8^\circ$) \Rightarrow w=1, ($8^\circ < \sigma_{\text{azim}} \leq 10^\circ$) \Rightarrow w=0.8, ($10^\circ < \sigma_{\text{azim}} \leq 12^\circ$) \Rightarrow w=0.5, ($12^\circ < \sigma_{\text{azim}} \leq 15^\circ$) \Rightarrow w=0.3, and ($15^\circ < \sigma_{\text{azim}}$) \Rightarrow w=0.2. If no direction of a track can be determined, the weight is zero and instead a 'quality letter' is given in the table. 'A' means almost certainly a hotspot but no track (*e.g.*, Etna or Tristan da Cunha), 'B' means perhaps a hotspot but not too certain (*e.g.*, Massif Central), and 'C' means most likely not a hotspot even though some characteristics may suggest one (*e.g.*, Jan Mayen). Those with 'C' are not listed in Table 1. The weight w has no

meaning in regards to the rate, only rate error bars indicate that.

SUPERSWELL REGION

The determination of azimuths and rates as described in the electronic supplement was generally quite straight forward, except in the central Pacific with its very large number of tracks, many very close together, and many of apparently short (~5-10 Ma) duration. In this section we summarize our findings in the Pacific superswell region, roughly defined as the region enclosed by the Easter, Marquesas, Samoa, and Foundation features. This region is marked by shallower-than-normal seafloor (by ~500 m), numerous volcanic chains, and a warmer-than-typical mantle (*e.g.* McNutt and Fischer, 1987; Sichoix *et al.*, 1998). The anomalous nature of this area has lent much support to non-plume models of mantle convection (the website <<http://www.mantleplumes.org/>> describes many of these models with discussions about them). We think the essence of these non-plume models is most clearly presented by Anderson (2005, page 44): "The plate hypothesis assumes that the upper mantle is near the melting point and is variable in fertility, temperature, and solidus temperature. A small change in temperature, volatile content, and composition can have a large effect on melt volumes for a near-solidus mantle. Plate and plate tectonic-induced perturbations can generate 'melting anomalies'." (The 'plate tectonic-induced perturbations' in this region being overall plate tension, with the volcanoes regarded as stress indicators.)

We think the geodynamic nature of this region is perhaps best interpreted as shown in Figure 4 of Courtillot *et al.* (2003) or Figure 14 of Davaille *et al.* (2003). An important variation of this is shown in Figure 2 of Jellinek *et al.* (2003) or Figure 4 of Gonnermann *et al.* (2004). In these figures, we see from shadowgraphs of narrow plumes rising from a hot bottom boundary layer that the bases and rising columns of plumes get swept toward the regions with the most uprising – there are thus many, many more plumes in a 'superswell' region. This general pattern is portrayed even more clearly, but even more schematically, in Figure 17 of Jellinek and Manga

(2004; reproduced here as our Figure 3.) Our interpretation of the superswell region is that a very large amount of upward transport from the core/mantle boundary region overwhelms the normal geothermal profile of the Earth and leads to consequences not present above narrow rising plumes. We think for almost all the mantle, asthenosphere (being brought up by plumes from the core/mantle boundary region) is warmer than the mantle below the asthenosphere; this excess of (potential) temperature makes the asthenosphere stable against convection from just below. (That is, a mid-ocean rise has no 2-D style mantle 'roll' rising from deep beneath it, rather the needed material flows in horizontally from asthenosphere supplied at the nearest plume.) But perhaps an extreme excess of a broad rising plume in the superswell region creates a mantle with the same (potential) temperature as asthenosphere, and instabilities that do not exist elsewhere can exist here. In any case, this is a very anomalous, very interesting region; understanding this will likely lead to a big advance in geodynamics.

DISCUSSION

What can we conclude from the information presented above and in the electronic supplement? First, we show two figures from our analysis which uses the observed directions of hotspot tracks in Table 1 to solve for motions of plates over a fixed mantle reference frame. From these we show how well a 'fixed reference frame' fits the tracks on all plates. After that, we will return to the 'superswell' problem.

The plate motion in a fixed reference frame was found in the following manner. The motions of the major plates are tied together using NUVEL-1A rotations (DeMets *et al.*, 1994). Solving for the three parameters of one plate, the motions of all plates are determined. We took a starting trial 3-parameters (ω_x , ω_y , ω_z) for the Pacific, used NUVEL-1A to compute the angular velocities of other plates and thus predict the azimuths of tracks at each hotspot in our data set, and then searched for the three parameters that minimized a misfit-measure. Our measure was

the sum of the weight of a given track times the absolute value of the difference between the observed azimuth and the computed azimuth (*i.e.*, minimized $\sum w_i \times |AZ_{iobs} - AZ_{ipred}|$).

(Almost any minimizing function would give essentially the same result. This scheme downplays outliers as extreme differences are not squared in the sum.) Azimuth-only data are all that are needed because the velocities get determined by the NUVEL-1A model – if the choice of pole position (of the Pacific) is correct but the angular velocity is wrong, tying to other plates would seriously mismatch the azimuths of motion there. (An azimuths-only scheme was used by Gripp and Gordon (2002) in one version of their solution, but then they included rate-data for their final HS3 model.) The advantage of azimuth-only data is azimuths are more accurately observed and there are no systematic errors as may be present in rate measurements. Many of the tracks are poorly dated, and K-Ar measurements may have unknown systematic errors. Also, how do you devise a weighting function to include a track with an accurate azimuth but poorly determined rate in with the other tracks? We have used azimuths only, and shall test the solution by comparing it with the measured rates. (A systematic comparison of the measured rates, and their error estimates, with model-predicted-rates is a major component of our paper-in-progress. Here we have only a visual comparison as shown in Figure 2b.)

An important concern is azimuths on the Pacific and Nazca plates are determined from 'recent' (0 to ~5 Ma) parts of the tracks whereas on the slower plates the azimuth is generally defined over a longer period of time (0 to ~10 Ma), and on some of the poorest defined tracks (Hoggar, Tibesti, Afar, Cape Verde, Kerguelen) over up to ~30 Ma. (The fast-moving Australian tracks are averaged over a longer period for a different reasons: (1) there are no seamounts in the Tasmantid chain younger than 5 Ma, and (2) the very straight-line alignment of the inland volcanics used to find the azimuth of the East Australian track range in age from 8 to 17 Ma.) However, several of the 'slow' tracks are quite narrowly defined in azimuth (Eifel, Canary, St. Helena, Martin Vaz, Fernando do Noronha, Yellowstone, Raton) and there is no obvious 'kink' in their tracks to suggest a significant long-term/short-term difference.

Figure 1 shows how the bootstrap method was used to estimate the uncertainty in the

lat/long/rate of the Pacific plate motion over the mantle. From the data table of 57 hotspots/weights/azimuths, we generated many synthetic data sets each with 57 values randomly selected from the actual data set. In these synthetic sets, some hotspots appear multiple times, some are omitted – it is a random, non-emptying selection. For each synthetic set, there is a search for the ω_x , ω_y , ω_z that minimizes the misfit-measure. To visualize this process, the lat/long of the best-fit for each synthetic set is plotted as a dot in Figure 1a. The average of all of these is the best pole for the original data set; the dispersion of points measures the error of this 'best-fit'. (No information on rates is displayed in Figure 1a.) The concentric ellipses are of sizes that contain 68%, 90%, and 95% of the 'points'; these show the confidence intervals. The figure was drawn with only 330 synthetic samples (many more were used to fix the orientation and sizes of the ellipses). With this smaller number you can see individual points instead of a blur, *e.g.* 14 points are outside the 95% confidence ellipse, very close to 5% of the total 330 points. The streaks and lines are not random variations; these occur because when a best-fit for a given synthetic set is calculated it is strongly influenced by which plates end up with many repeats of a datum and which end up with very few (or none).

Figure 1b is a vertical cross-section in angular velocity space through the center of the 'ellipsoid' of bootstrap solutions of ω_x , ω_y , ω_z . The component ω_y' is parallel to the best-fit vector and shows the magnitude of the rotation rate; ω_x' is perpendicular to this and acts to change the orientation of the angular velocity in the E-W direction. The scale of Figure 1b was chosen such that a change in ω_x' will measure the same horizontal distance as the corresponding change in longitude in Figure 1a. Again, ellipses are drawn that would contain 68%, 90%, and 95% of the points if the points fell off as a normal distribution. If the pole position is a little west, closer to the Pacific plate, its angular velocity is greater. The combination of radius and angular velocity interact with each other in a manner that keeps the linear velocities of points in the Pacific about the same for small changes in the pole position. [this para is unintelligible. What do you mean by “vertical cross-section”? Please redraft]

Figure 2 compares our model with the observations listed in Table 1. The top panel shows the predicted azimuths (black lines) of our model and observed azimuths (gray lines). The agreement with the azimuth data is quite remarkable. Only three locations have notable differences between the observed and model directions: Comores, Marquesas, and Louisville. [This is going to puzzle readers. Many others fit badly, e.g., Balleny, Scott and Canary] We have no real guess why the Comores track is as it is, for Marquesas we have guessed interaction with a nearby major fracture zone deflected the track, and for Louisville we have chosen the azimuth of the recent trend of the Hollister Ridge and not the northern position/track used by others (and which generates the long-term trend of the entire Louisville chain). The bottom part of the figure shows arrows whose lengths are proportional to velocity. It shows the model velocities (black arrows) and the observed velocities (gray arrows). If a velocity has not been observed, a gray line without an arrowhead is drawn with the direction of the observed azimuth. All high velocities are in the Pacific or Australian regions, all other plates have very slow velocities over the mantle. The fit to the velocity data is not as good as above. On a number of tracks (Caroline, Guadalupe, Macdonald, Arago, Society, Easter, Canary, Reunion, and Crozet) the observed rate is significantly higher than the model rate. (Note of these, only Canary and Easter have rates based on $^{40}\text{Ar}/^{39}\text{Ar}$ dating, rates for the other seven are based on K-Ar.) We have come to the conclusion that the azimuth data set is a much cleaner set and the velocity set less reliable. Velocities are harder to determine – late stage volcanism, delayed volcanism getting through the lithosphere, and argon-loss in samples due to small degrees of weathering all systematically shift the age 'too young' (and the rate 'too high'). The most striking feature of Figure 2b is the contrast between the very high velocities in the Pacific area and very small, even near-zero, velocities on the other plates. Our model not only duplicates the very slow velocities on these plates but even correctly predicts the azimuths of tracks on these plates.

Our pole position at 59.33°N , 85.10°W is very similar to that of earlier papers (e.g., Minster and Jordan, 1978; Gripp and Gordon, 1990; Gripp and Gordon, 2002). Our confidence ellipse is smaller, but that is a minor difference resulting from the use of a larger data set. What is really

different is the rate of angular velocity – ours (89.20 mm/yr or $-0.8028^\circ/\text{yr}$) is significantly less than, say, that of Gripp and Gordon (2002). With this slower rotation about essentially the same pole, the predicted directions of motion of all other plates fits the observed azimuths of their hotspots tracks. If the angular velocity of the Pacific is 'too high', it adds a westward component to the motion of all plates which can result in up to $\sim 180^\circ$ difference between predicted and observed tracks on very slow moving plates. We tried several variations based on the data in Table 1. In one case, we used only the 19 very best determined azimuths (those with weight '1'), in another case we used the 34 'very good' azimuths (those with weights 1 or 0.8), and in a third case we used all 57 azimuths but gave them all a weight of '1' irrespective of the w listed in the table. These cases gave solutions $59.38^\circ\text{N}, 83.20^\circ\text{W}, 87.40\text{ mm/yr}$; $59.01^\circ\text{N}, 83.45^\circ\text{W}, 87.96\text{ mm/yr}$; and $59.66^\circ\text{N}, 87.47^\circ\text{W}, 89.77\text{ mm/yr}$ respectively. All of these cases fell within the 90% confidence ellipse shown in Figure 1a. (The error ellipses of these other cases were all larger than our 'best' solution shown in Figure 1a, generally by a factor between 1.5 and 2.)

Then we chose a data set consisting of the 37 tracks that were 'non-Pacific', *i.e.*, omitting those tracks on the Pacific, Nazca, or Cocos plates. This data set gave a solution of $59.32^\circ\text{N}, 85.00^\circ\text{W}, 89.18\text{ mm/yr}$ – almost identical to our solution using all the data. Thus we find no difference from the pole of non-Pacific hotspots and the pole using all the tracks. Next we chose a data set where only the 20 tracks on the Pacific, Cocos, or Nazca plates were used. These gave a solution of $61.1^\circ\text{N}, 77.5^\circ\text{W}, 83.2\text{ mm/yr}$ but with very large uncertainties: the 95% ellipse had a semi-major axis of 24 arc-deg, semi-minor 8 arc-deg, with the long-axis along an azimuth of 069° . (This 'Pacific only' pole is marked with a cross labeled 'P-O' in Figure 1a.) This large uncertainty was expected from the azimuth-only technique; with the data essentially all on the same plate, the lines perpendicular to the tracks are all near parallel – no cross-cutting constraints to refine the position in the 'long-direction'. We would need velocity *vs.* distance data to pin down the best pole on this long 'smear', just as both fracture zone trends and spreading rates are needed to accurately fix a pole for the relative motion between two plates. We then chose a slightly larger data set, the 20 'Pacific' tracks above plus Yellowstone and Raton on the North

American plate and the East Australian, Tasmanid, and Lord Howe tracks on the Australian plate (reasoning these are nearby and might be part of a 'Pacific set'). This gave a solution of 60.8°N , 83.8°W , 89.2 mm/yr with smaller but still large uncertainties, for 95%, $a= 12\text{ arc-deg}$, $b= 7\text{ arc-deg}$, azimuth= 040° . (This 'Pacific' plus North America plus Australia pole is marked with a cross labeled 'PNA' in Figure 1a.) However, there was no need to find the pole for 'Pacific only' motion ourselves. The papers by Minster and Jordan (1978) and Gripp and Gordon (1990; 2002) have already done this. The Minster and Jordan (1978) and Gripp and Gordon (1990) papers use only data from the Pacific-Cocos-Nazca plates plus only one other bit of data – the azimuth of the Yellowstone track in North America. The Gripp and Gordon (2002) paper uses data from the Pacific area and Yellowstone plus only one other bit of data – the azimuth of the Martin Vaz/Trindade trend on the South American plate. These three poles are shown in Figure 1a, marked MJ78, GG90, and GG02. They are all within $\sim 3\text{ arc-deg}$ of our pole that best-fits the 'non-Pacific' set: the 37 tracks not on the Pacific or Cocos or Nazca plates. (Recall the 'non-Pacific' pole is practically on top of our pole that best-fits all 57 tracks.)

We conclude, for present-day motion, that a single reference frame fits the entire world – the hotspots as a group in the 'Pacific' do not drift relative to a group centered on 'Africa'. The various poles for 'Pacific' are $\sim 3^{\circ}$ from our pole for 'non-Pacific', just outside our error ellipse but our pole is well within the larger error ellipses of these three earlier studies. The rates about these poles are different; our rate is $\sim 89\text{ mm/yr}$, theirs average about 20% higher ($\sim 110\text{ mm/yr}$). If the hotspots on opposite sides were to drift relative each other, we find it very strange they would both move about the same pole but have different rates about this pole – why not a totally different pole if one side moves relative to the other? Note also our slower rate is close to the average rate of Pacific motion for the past 47 Ma – the higher rate of other models needs to have been much slower earlier or the Pacific tracks would get to the 'Emperor bend' too soon. Our conclusion is earlier studies have chosen a 'too high' velocity, biased by systematics in the rate measurements of the hotspot tracks.

Could the rates of track migration on the Pacific plate be high because the mantle and hotspot

pipes themselves are being pushed away from the Japan/Marianas centers of subduction? That is, the high velocity measurements in the Pacific are correct but there is this added component as explained in several papers by Bernhard Steinberger (*e.g.*, Steinberger, 2000; Steinberger and O'Connell, 1998; 2000). We think this pipe-drift effect is real, but that the rates of hotspot drift are not ~ 20 mm/yr as needed to explain the difference between our model and the earlier models. In a simple mass balance, a 200-km-thick slab descending into the lower mantle at 100 mm/yr creates a volume flux that can be matched by a 2000-km-thick slab of lower mantle moving horizontally at 10 mm/yr, or, with half the flow going in each direction, at ~ 5 mm/yr. This effect might have strong influence at some sites (say, Caroline), but could not cause all the tracks in the Pacific to drift west-to-east at the ~ 20 mm/yr needed to reconcile the earlier models to ours. Further, the ~ 5 mm/yr is probably on the high side – even 5 mm/yr drift of hotspots would play havoc with the strikingly good model-to-data fit of azimuths on the slower plates.

SOME INFERENCES

Given this background, that we find strong support for a model of rigid plates over a fixed mantle reference frame, we wish to discuss two issues that came up during our compilation of the data for each track. The first is the closeness of pairs of hotspots, the second is the 'superswell problem'.

There are a number of hotspots that are very near other hotspots – so close it suggests they cannot be independently anchored deep in the mantle at the core-mantle boundary. In particular, the pairs Tristan/Gough, Madeira/Canary, Eifel/Massif Central, Kerguelen/Heard, Eastern Australia/Tasmantid, Easter/Crough, and Cobb/Pratt-Welker (Bowie). A possible explanation for this without changing the fixity of hotspots is as follows. Suppose in the initial, flood-basalt stage of a plume, a large 'pipe' 300 km across develops to rapidly carry the large volume to the surface. The excess temperature of the ascending plume causes 'zone refinement' in the mantle surrounding the pipe. The higher temperature and increased diffusion rate 'sucks out' volatiles

from the surrounding mantle, leaving a wall a few tens of kilometers thick. Without the volatiles, this wall is 'tougher' than normal mantle. Then, as the large plume flux fades away, the 300 km diameter tube is too large for the flux it carries. The tube starts to collapse, flattening into an elongate elliptical cross-section. As the upward flux continued to decrease, opposite sides of the tube might touch each other sealing off the center. But the two distal portions would remain open because the 10+ km thick tough rind flexes with a minimum radius, not deforming into a tight crease that would seal the tips. If something like this were so, what might be tests? Three observations might be: (1) the pairing would occur long after a flood basalt stage, (2) at the very end of a plume's life, the flux might become too low to supply two conduits and one might disappear by starvation, and (3) the plane between the two 'tips' would be oriented perpendicular to the maximum horizontal compressive stress in the lower mantle.

How can the superswell region, with its (1) shallower-than-normal seafloor, (2) numerous short volcanic chains that appear to turn on/turn off with time scales of ~10 Ma rather than the ~100 Ma typical of many hotspots, and (3) a warmer-than-typical mantle (see the section 'Superswell Region' located in the main text just after the discussion on the Marquesas Islands for details), be reconciled with our model of a global, mantle-fixed reference frame? We assume a very, very weak asthenosphere that almost completely decouples the plates from the mantle below. (This decoupling is less complete beneath old parts of continents, consequently plates with large areas of shield/platform move slower over the mantle than do largely 'oceanic' plates.) In a recent paper on mantle viscosity, Mitrovica and Forte (2004, Fig. 1c,d) find a low-viscosity channel below the lithosphere, a higher viscosity just beneath the asthenosphere, and then a much higher viscosity in the lower mantle (until very near the core-mantle boundary). In averages we made when we re-chose the depth of boundaries between regions, we get from their Figures 1c and 1d the following: $\eta = 5 \times 10^{19}$ Pa-s between 100 km and 300 km, $\eta = 5 \times 10^{20}$ Pa-s between 300 km and 660 km, and $\eta \approx 2 \times 10^{22}$ Pa-s in the lower mantle. This general pattern, with a low-viscosity asthenosphere channel and higher-viscosity lower mantle and with approximately the same ratios between high and low viscosities, was also found by Panasyuk

and Hager (2000, Fig. 5a,b). In our analysis of horizontal flow in an asthenospheric channel, we found an average viscosity of the asthenosphere of 7×10^{18} Pa-s (Yamamoto *et al.*, 2007, caption to Fig. 16). (In this analysis, we assumed the base of the asthenosphere was at 300 km – the thickness of the asthenosphere was ~ 200 km, varying slightly as the lithosphere thickened with age. If the asthenosphere viscosity were greater than 7×10^{18} Pa-s, there would be too much 'pile up' and corresponding lift of the seafloor because of the pressure gradient created by plate drag as the Pacific moves westward toward the Mariana and Japan trenches.)

Using these viscosities and thicknesses ($\sim 1 \times 10^{19}$ Pa-s in a 200 km thick asthenosphere, $\sim 5 \times 10^{20}$ Pa-s between ~ 400 km to 660 km, and $\sim 2 \times 10^{22}$ Pa-s in a ~ 2000 km thick lower mantle), we get roughly the following. If a hotspot source is well anchored near 660 km at the base of the transition zone, its 'drift' relative to the 'fixed' frame would be only $\sim 1/20$ of the horizontal motion of the plate above (assuming uniform shear stress in the layers). If it is anchored at the base of the mantle, its drift would be even less – determined by horizontal flow in the lower mantle forced by 'mass balance' of what is being injected in at subduction zones. (However, much of the horizontal transport in the lower mantle could be very high velocities in the low-viscosity D" layer and not slow horizontal velocities distributed throughout the lower mantle.) The fixity of hotspots has been one of the main arguments favoring their sources being near the core-mantle boundary. We have shown in the bulk of this paper that this fixity is even stronger than previously thought, but if this fixity is due to a near-inviscid asthenosphere decoupling the plates from all mantle below, this is no longer a reason to place the sources at the base of the mantle. However we think there are other arguments favoring the deep origin of plumes.

In our model, all asthenosphere is created by plumes bringing material up from D". This is a very large flux: the total upward flow in all plume pipes is ~ 300 km³/yr – the same as the downward flux of all slabs. The asthenosphere is very hot – it is the temperature of D" minus only the adiabatic effect as the plume rises to asthenosphere depth. The subducting slabs carry 'coldness' into the mantle. These are gradually warmed up by conduction inward from the

surrounding mantle (extracting heat from a larger volume), by internal radioactivity over their trip-time of order billion years, plus the added input for the short time material is in D" before coming back to the asthenosphere. This pattern of convection would produce an asthenosphere hotter than the mantle below it. Downward conduction of heat from the asthenosphere would make an isothermal temperature gradient in the transition-zone region between the base of the asthenosphere and the 660-km discontinuity (and somewhat below the 660-km discontinuity, or at least reduce the temperature increase with depth to below the adiabatic gradient. Thus the mode of convection we are suggesting would act as an on/off switch – if the plumes bring up enough hot material from D" depths to make a hot asthenosphere, then this turns off all other convection from the mid-mantle/660-km discontinuity into the upper mantle. That is, adiabatic cooling of material starting from mid-mantle or 660-km depths would be cooler than the shallower levels it would be trying to reach and so such modes of convection (such as rising from below the EPR to supply the spreading ridge with material) would be turned off. This model requires 'enough' material be brought up by plumes and that the material spread out easily from where there are 'sources' of asthenosphere (above plumes) to where there are 'sinks' of asthenosphere (mid-ocean ridges). We do not know how much is 'enough', but once this limit is reached, it becomes the only mode of convection.

We think the plate-tectonic cycle adjusts its rate to equal what is brought up by plumes. If plume rates were to decrease, the asthenosphere would thin, plate drag would increase, and subduction rates slow down. Contrariwise, if plumes were more vigorous, plate drag would decrease and movement toward subduction zones would be faster. There may be cycles of fluctuations tens of millions of years long in this. For example, at the time of a flood basalt the asthenosphere may temporarily increase in volume, the asthenosphere then thinning as this excess is used up (the Cretaceous super-cycle may be such a case) – but the long-term rate is set by the plumes. (Many consequences of this pattern of flow are explored in Yamamoto *et al.*, this volume.)

This pattern of flow can efficiently extract heat from the Earth's interior and set the rate for

plate tectonics, but how can it be applied to the superswell region? Why would a small area of the Pacific (only 5% of the Earth's surface) have a quarter of the world's hotspot tracks? A slightly larger region (~10% of the Earth) on the African side has another quarter of all hotspots. If the long-term convection scheme remains more or less the same for some long period of time, this could 'sweep' the rising plumes into a central region – the pattern shown schematically in Figure 3 (adapted from Figure 17 in Jellinek and Manga, 2003), is a highly schematicized interpretation of the plume/tank experiments shown in Figure 4 of Gonnermann *et al.*, 2004.) This same idea is nicely illustrated in Figure 11 of Steinberger and O'Connell (1998) and is clearly stated on page 76 of Steinberger's thesis (Steinberger, 1996): "This raises another possibility - plumes might be stationary where they are, not because flow in the mantle is so slow, but because they already have been advected into large-scale stationary upwellings in the lower mantle, ...".

Convective overturn is what removes interior heat by bringing mantle close to the top surface where its heat is lost through the surface by conduction. We think the asthenosphere is hotter than mantle beneath it, cutting off any upwelling from the transition zone into the asthenosphere except for where there are rising plumes and possibly the superswell region as discussed below. This does not mean there are no up and down motions in the mantle except sinking slabs and rising plumes. Rather any secondary interior flow induced by denser slabs and buoyant plumes will not lead to heatloss through the surface – in this sense slow interior flow is only of secondary importance to Earth's convective heat transport.

For most of the Earth, a 'hotspot' at the surface is an indication of a plume rising from deep. The exception is in the superswell region. If a plume, or group of plumes, remains in one place in the mantle for 100's of millions of years, the outward conduction of heat from the rising pipe would spread out into the surrounding mantle. If it conducts outward ~100 km in 100 Ma; it would conduct outward ~300 km in 1 b.y. If rheology depends on temperature and volatile content, the high temperature alone would make the mantle surrounding a pipe less viscous than 'average' mantle, but a 'zone-refining' effect as discussed above would increase the viscosity of

the region around a pipe. The net result may be the mantle around a pipe is 'hotter' but not significantly less viscous than other parts. Thus in the superswell region, the usual 'stable' geotherm pattern (where asthenosphere is hotter than mantle below) is overwhelmed. Here relatively shallow convective instabilities could occur as temperatures at the 660-km-discontinuity and mantle above this might be hotter than asthenosphere (because of the long-term outward conduction of heat into the mantle from the stable pipes). Short-term instabilities could then rise into the asthenosphere, creating short-lived tracks. In our model of viscosity structure of the upper mantle (from Mitrovica and Forte, 2004; Panasyuk and Hager, 2000; Yamamoto *et al.*, 2007) the mantle between ~400-660 km is considerably more viscous than asthenosphere and would have small velocities compared to fast plate motion. Thus observed tracks at the surface would be all near-parallel to plate motion and all have migration rates very close to the velocity of the plate – rooted in the lower transition zone would be nearly as 'fixed' as rooted at the core-mantle-boundary, just not have the long lifetime. A scheme like this (the main features of which could be validated with numerical modeling) reconciles the model of plumes rising from the core-mantle boundary as the primary pattern of mantle convection with the conundrum of so many hotspots, many short-lived, and many close together, as was forcefully argued in the book 'Plates, Plumes, and Paradigms' (Foulger *et al.*, 2005).

ACKNOWLEDGEMENTS

[Appropriate in electronic supplement] WJM thanks the Department of Earth and Planetary Sciences at Harvard for welcoming him as a visiting researcher. For the tracks on land, the map collection at the Princeton University library was invaluable – for tracks in the oceans, the synthetic-bathymetry of W. H. F. Smith and D. T. Sandwell (version 7.2) was our primary source. Blowup plots of the bathymetry defining the ocean tracks were easy to make because of the GMT software of P. Wessel and W. H. F. Smith (1998), and we especially thank W.H.F.S. for showing us a work-around to a plotting difficulty we encountered. Ajoy Baksi showed us

how to use the metadata to evaluate the accuracy of an age date. We thank Gill Foulger, Richard Gordon, Dietmar Müller, and Bernhard Steinberger for their thoughtful reviews, which added significantly to our manuscript. WJM thanks the Alexander von Humboldt Foundation and Princeton University and JPM thanks the National Science Foundation and Deutsche Forschungsgemeinschaft (DFG) for support during the course of this work.

REFERENCES CITED

(An additional 289 references referring to specific tracks are in the electronic supplement.)

- Anderson, D.L., 2005, Scoring hotspots: the plume and plate paradigms, *in* Foulger, G.R., Natland, J.H., Presnall, D.C., and Anderson, D.L., eds., *Plates, plumes, and paradigms: Geological Society of America Special Paper 388*, p. 31-54.
- Courtillot, V., Davaille, A., Besse, J., and Stock, J., 2003, Three distinct types of hotspots in the Earth's mantle: *Earth and Planetary Science Letters*, v. 205, p. 295-308.
- Davaille, A., Le Bars, M., and Carbonne, C., 2003, Thermal convection in a heterogeneous mantle: *Comptes rendus – Geoscience*, p. 335, p. 141-156.
- Foulger, G.R., Natland, J.H., Presnall, D.C., and Anderson, D.L., eds., 2005, *Plates, plumes, and paradigms: Geological Society of America Special Paper 388*, 881 p.
- Gonnermann, H.M., Jellinek, A.M., Richards, M.A., and Manga, M., 2004, Modulation of mantle plumes and heat flow at the core mantle boundary by plate-scale flow: results from laboratory experiments: *Earth and Planetary Science Letters*, v. 226, p. 53-67.
- Gripp, A.E., and Gordon, R.G., 1990, Current plate velocities relative to the hotspots incorporating the NUVEL-1 global plate motion model: *Geophysical Research Letters*, v. 17, p. 1109-1112.
- Gripp, A.E., and Gordon, R.G., 2002, Young tracks of hotspots and current plate velocities: *Geophysical Journal International*, v. 150, p. 321-361.
- Jellinek, A.M., and Manga, M., 2004, Links between long-lived hotspots, mantle plumes, D",

- and plate tectonics: *Reviews of Geophysics*, v. 42, no. 3, doi:10.1029/2003RG000144, 35 p.
- Jellinek, A.M., Gonnermann, H.M., and Richards, M.A., 2003, Plume capture by divergent plate motions: implications for the distribution of hotspots, geochemistry of mid-ocean ridge basalts, and estimates of the heat flux at the core-mantle boundary: *Earth and Planetary Science Letters*, v. 205, p. 361-378.
- McNutt, M.K., and Fischer, K.M., 1978, The South Pacific superswell, *in* Keating, B.H., Fryer, P., Batiza, R., and Boehlert, G.W., eds., *Seamounts, islands, and atolls: American Geophysical Union Geophysical Monograph 43*, p. 25-34.
- Minster, J.B., and Jordan, T.H., 1978, Present-day plate motions: *Journal of Geophysical Research*, v. 83, p. 5331-5354.
- Mitrovica, J.X., and Forte, A.M., 2004, A new inference of mantle viscosity based upon joint inversion of convection and glacial isostatic adjustment data: *Earth and Planetary Science Letters*, v. 225, p. 177-189.
- Sichoix, L., Bonneville, A., and McNutt, M.K., 1998, The seafloor swells and Superswell in French Polynesia: *Journal of Geophysical Research*, v. 103, p. 27123-27133.
- Steinberger, B.M., 1996, Motion of hotspots and changes of the Earth's rotation axis caused by a convecting mantle (Ph.D. thesis): Cambridge, MA, Harvard University, 203 p.
- Steinberger, B.M., 2000, Plumes in a convecting mantle: models and observations for individual hotspots: *Journal of Geophysical Research*, v. 105, p.11127-11152.
- Steinberger, B., and O'Connell, R.J., 1998, Advection of plumes in mantle flow: implications for hotspot motion, mantle viscosity and plume distribution: *Geophysical Journal International*, v. 132, p. 412-434.
- Steinberger, B., and O'Connell, R.J., 2000, Effects of mantle flow on hotspot motion, *in* Richards, M.A., Gordon, R.G., and van der Hilst, R.D, eds., *The history and dynamics of global plate motions: American Geophysical Union Geophysical Monograph 121*, (Washington, American Geophysical Union), p. 377-398.
- Wessel, P., and Smith, W.H.F., 1998, New improved version of Generic Mapping Tools

released: Eos (Transactions, American Geophysical Union), v. 79, 579. see also
<http://gmt.soest.hawaii.edu/> (accessed 15 May, 2006)

Yamamoto, M., Phipps Morgan, J., and Morgan, W.J., 2007, Global plume-fed asthenosphere flow: motivation and model development: *this volume*.

FIGURE CAPTIONS

Figure 1. Bootstrap solution pole positions for present-day Pacific plate motion in the fixed mantle reference frame based on the data set in Table 1. The scatter of the bootstrap solutions shows the error in determining the average; 68%, 90%, and 95% confidence ellipses are shown. The best solution is 59.33°N, 85.10°W with an angular velocity that produces 89.20 mm/yr at its 'equator'. (a) The 95% confidence ellipse of the pole position has parameters a : 2.11 arc-deg, b : 1.50 arc-deg, azimuth: 109.2 deg. (b) A 'vertical' slice in angular velocity space shows magnitude of rotation rate versus longitude. The component $\omega y'$ is parallel to the magnitude; $\omega x'$ changes the direction of the vector in the E-W direction. The scale is set so horizontal distance here is approximately the same as the longitude scale in part (a). Angular velocity is less if the pole position is farther from the Pacific (and *vice versa*), minimizing the change in linear velocity of points in the Pacific. The black circles and crosses marked MJ78, GG90, GG02, P-O, and PNA mark locations of other solutions discussed in the text.

Figure 2. (a) Thick gray lines with constant length show observed azimuths of hotspot tracks and thin black lines show predicted azimuths for each entry in Table 1. (b) Here the length of each arrow is proportional to velocity. Black arrows show predicted velocities and gray arrows (with arrowheads) show observed velocities. If the velocity of a track could not be

determined, a gray line with no arrowhead is drawn in the direction of the observed azimuth (with a length the same as the model velocity).

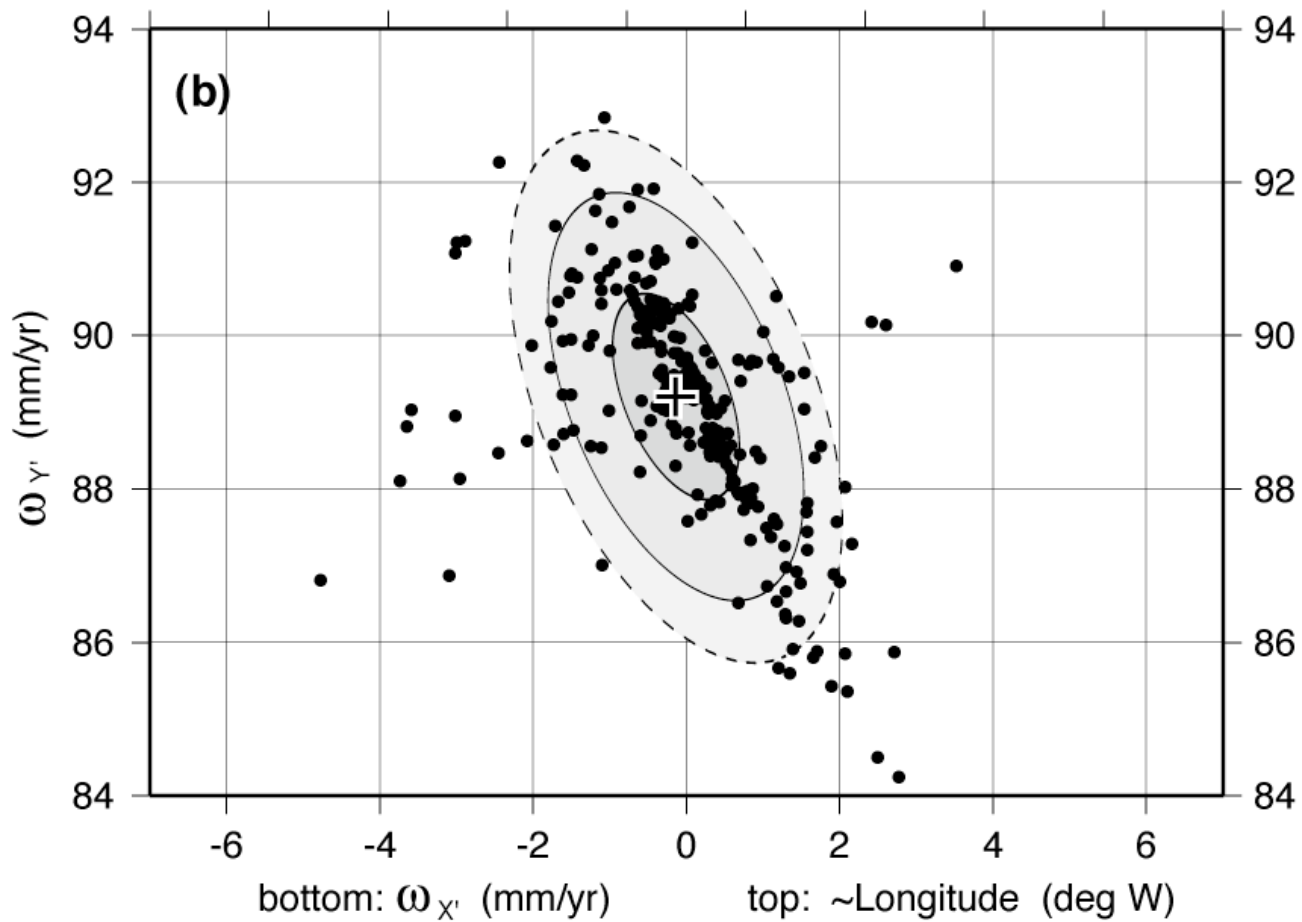
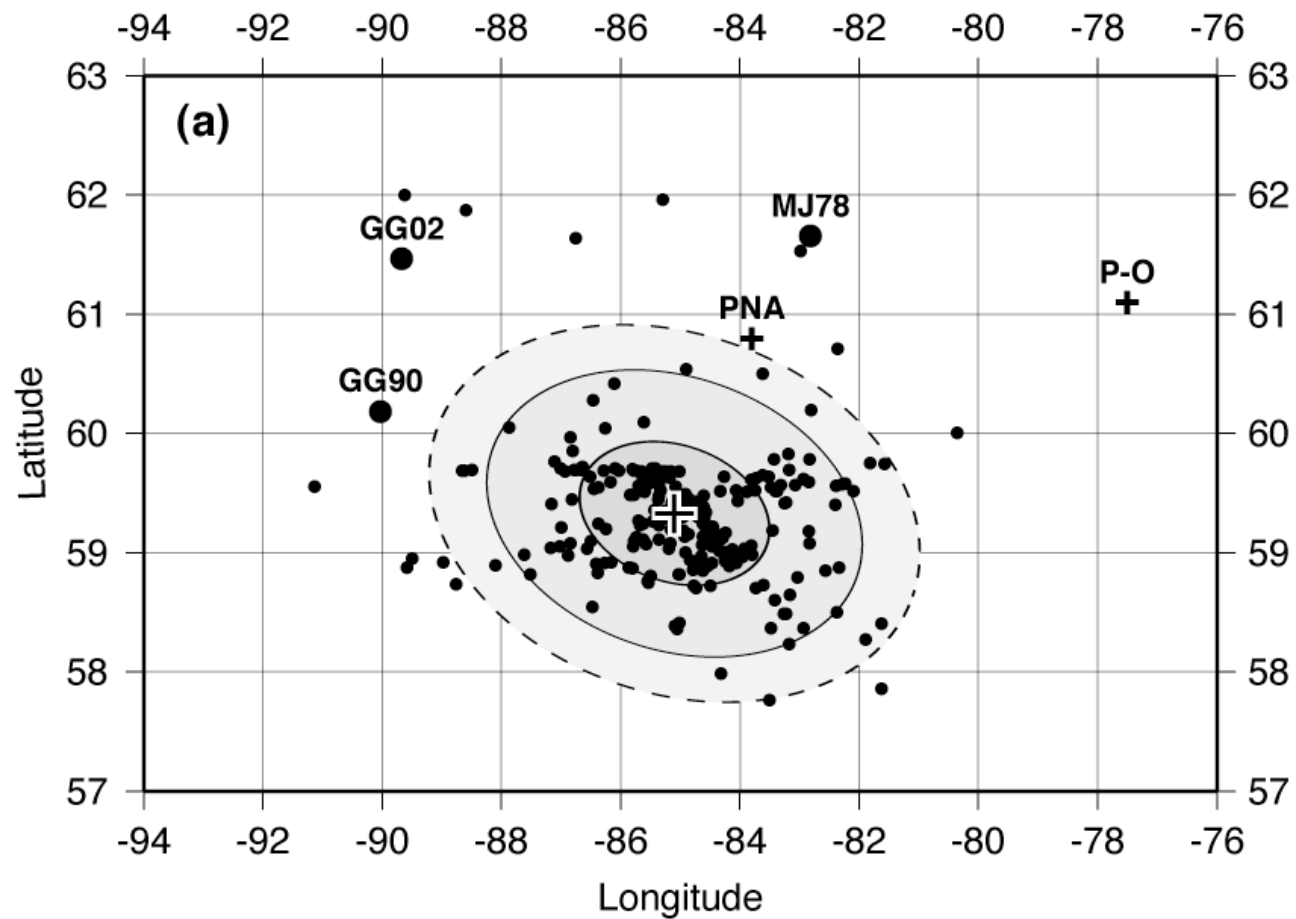
Figure 3. Schematic diagram (from Jellinek and Manga, 2004) illustrating how long-term subduction in fixed places (here the Andes and Western Pacific) could push/concentrate the plumes into the superswell regions.

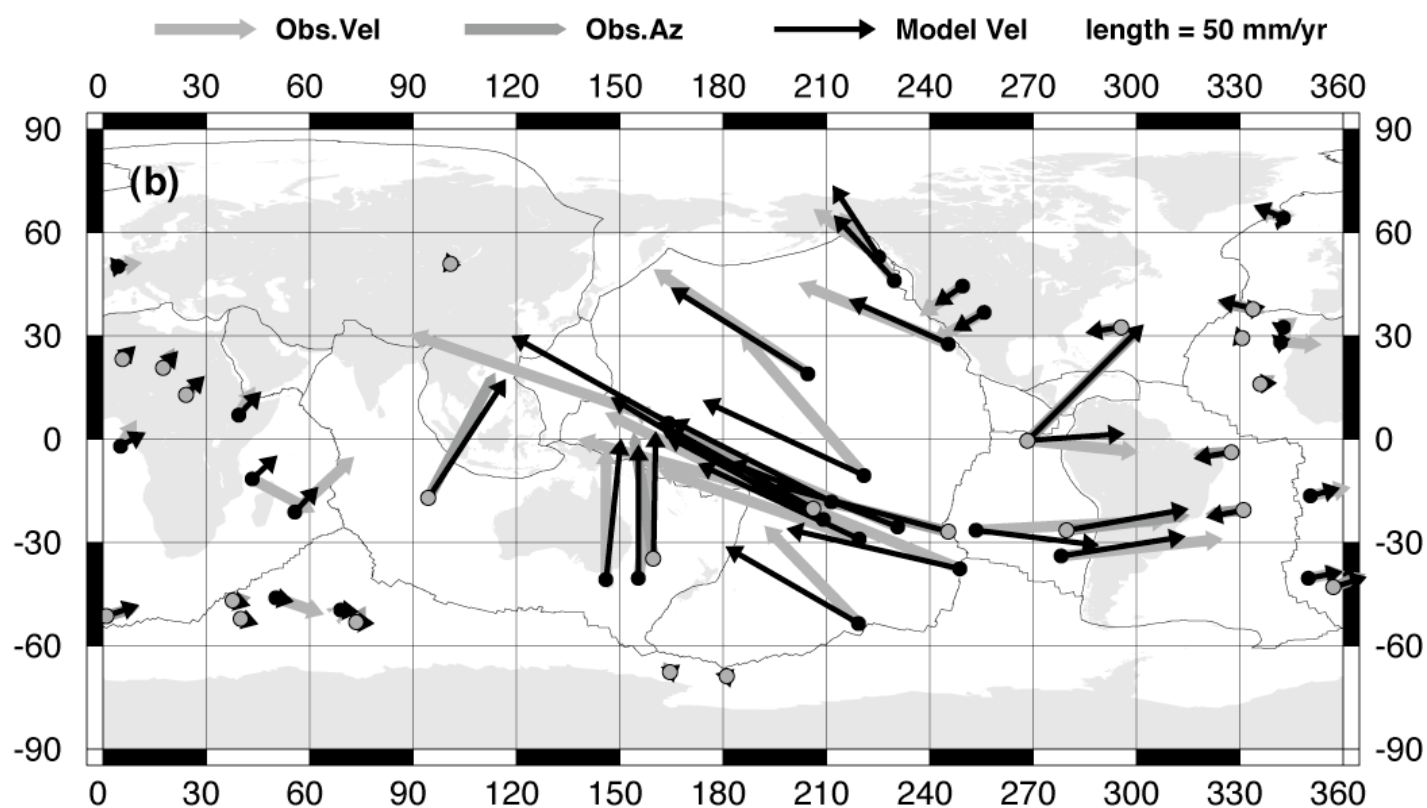
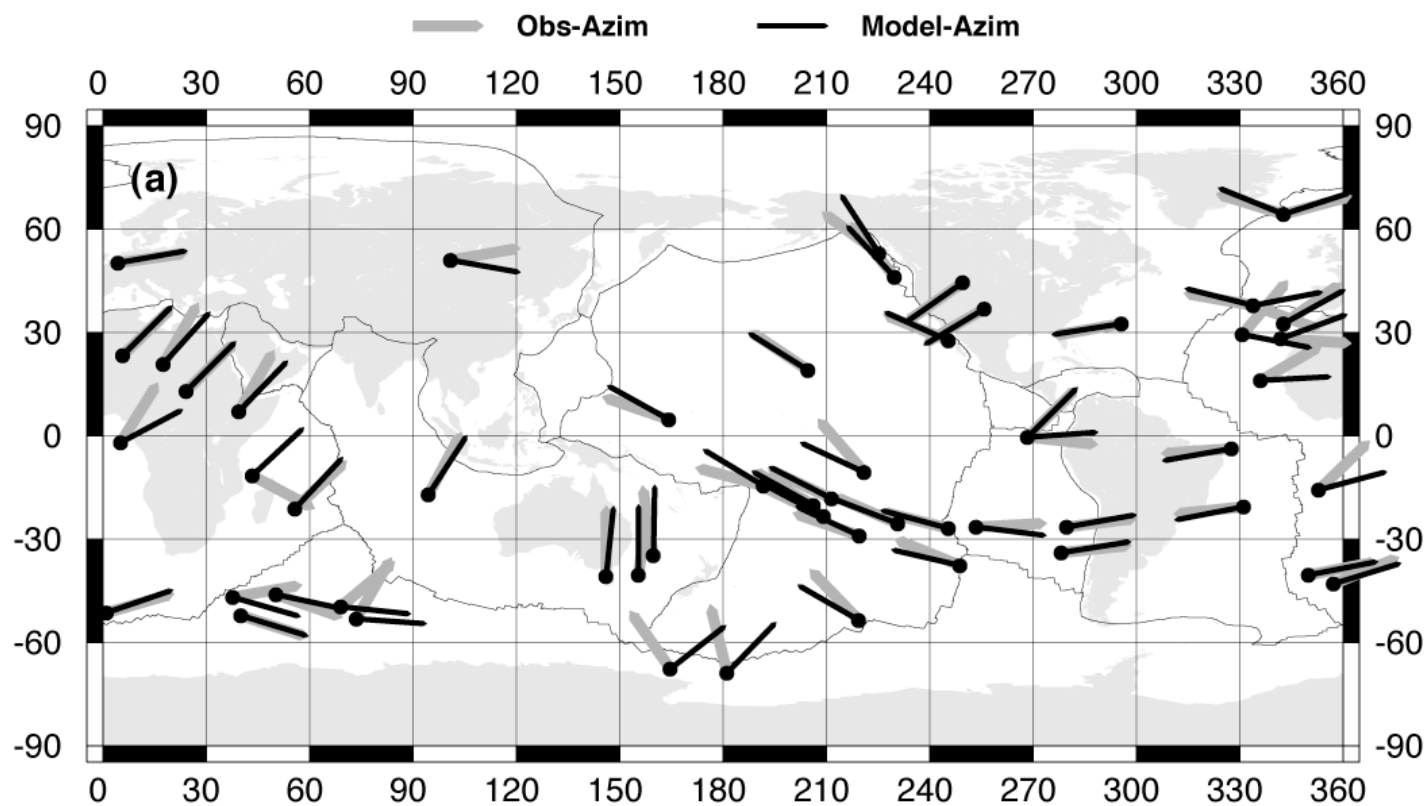
TABLE 1. AZIMUTH AND RATE OF EACH TRACK

HOTSPOT	PLATE	Lat (°N)	Long (°E)	Weight	Azobs (°)	± (°)	Vobs (mm/yr)	± mm/yr	Azmdl (°)	Vmdl (mm/yr)
Eifel	eu	50.2	6.7	1.0	082	±8	12	±2	080	5
Iceland	eu	64.4	-17.3	0.8	075	±10	5	±3	072	3
Azores	eu	37.9	-26.0	0.5	110	±12	N.D.*	N.D.	079	6
MassifCentral	eu	45.1	2.7	B	N.D.	N.D.	N.D.	N.D.	081	5
Etna	eu	37.8	15.0	A	N.D.	N.D.	N.D.	N.D.	083	6
Baikal	eu	51.0	101.0	0.2	080	±15	N.D.	N.D.	100	5
Hainan	ch	20.0	110.0	A	000	±15	N.D.	N.D.	N.D.	N.D.
Hoggar	af	23.3	5.6	0.3	046	±12	N.D.	N.D.	045	9
Tibesti	af	20.8	17.5	0.2	030	±15	N.D.	N.D.	042	11
JebelMarra	af	13.0	24.2	0.5	045	±8	N.D.	N.D.	045	13
Afar	af	7.0	39.5	0.2	030	±15	16	±8	044	16
Cameroon	af	-2.0	5.1	0.3	032	±3	15	±5	062	14
Madeira	af	32.6	-17.3	0.3	055	±15	8	±3	061	4
Canary	af	28.2	-18.0	1.0	094	±8	20	±4	070	5
GreatMeteor	af	29.4	-29.2	0.8	040	±10	N.D.	N.D.	101	4
CapeVerde	af	16.0	-24.0	0.2	060	±30	N.D.	N.D.	087	8
StHelena	af	-16.5	-9.5	1.0	078	±5	20	±3	075	15
TristanDaCunha	af	-37.2	-12.3	A	N.D.	N.D.	N.D.	N.D.	080	17
Gough	af	-40.3	-10.0	0.8	079	±5	18	±3	079	17
Vema	af	-32.1	6.3	B	N.D.	N.D.	N.D.	N.D.	067	17
Discovery	af	-43.0	-2.7	1.0	068	±3	N.D.	N.D.	073	17
Shona	af	-51.4	1.0	0.3	074	±6	N.D.	N.D.	071	17
Reunion	af	-21.2	55.7	0.8	047	±10	40	±10	043	17
Comores	af	-11.5	43.3	0.5	118	±10	35	±10	047	17
Kilimanjoro	af	-3.0	37.5	B	N.D.	N.D.	N.D.	N.D.	047	16
Karisimbi	af	-1.5	29.4	B	N.D.	N.D.	N.D.	N.D.	049	16
MtRungwe	af	-8.3	33.9	B+	N.D.	N.D.	N.D.	N.D.	049	16
Marion	an	-46.9	37.6	0.5	080	±12	N.D.	N.D.	106	9
Crozet	an	-46.1	50.2	0.8	109	±10	25	±13	102	9
Ob-Lena	an	-52.2	40.0	1.0	108	±6	N.D.	N.D.	107	9
Kerguelen	an	-49.6	69.0	0.2	050	±30	3	±1	096	9
Heard	an	-53.1	73.5	0.2	030	±20	N.D.	N.D.	094	9
Balleny	an	-67.6	164.8	0.2	325	±7	N.D.	N.D.	052	6
Scott	an	-68.8	-178.8	0.2	346	±5	N.D.	N.D.	044	5
Erebus	an	-77.5	167.2	A	N.D.	N.D.	N.D.	N.D.	037	4
Peter_I	an	-68.8	-90.6	B	N.D.	N.D.	N.D.	N.D.	124	1
MartinVaz	sa	-20.5	-28.8	1.0	264	±5	N.D.	N.D.	259	19
FernandoDoNoron	sa	-3.8	-32.4	1.0	266	±7	N.D.	N.D.	260	19
Ascension	sa	-7.9	-14.3	B	N.D.	N.D.	N.D.	N.D.	257	19
Guyana	sa	5.0	-61.0	B	N.D.	N.D.	N.D.	N.D.	266	18
Iceland	na	64.4	-17.3	0.8	287	±10	15	±5	292	16
Bermuda	na	32.6	-64.3	0.3	260	±15	N.D.	N.D.	261	18
Yellowstone	na	44.5	-110.4	0.8	235	±5	26	±5	235	17
Raton	na	36.8	-104.1	1.0	240	±4	30	±20	239	18
Azores	na	37.9	-26.0	0.3	280	±15	N.D.	N.D.	284	18
Anyuy	na	67.0	166.0	B-	N.D.	N.D.	N.D.	N.D.	157	7
LordHowe	au	-34.7	159.8	0.8	351	±10	N.D.	N.D.	001	63
Tasmantid	au	-40.4	155.5	0.8	007	±5	63	±5	000	66
EasternAustr	au	-40.8	146.0	0.3	000	±15	65	±3	006	70
Cocos-Keeling	au	-17.0	94.5	0.2	028	±6	N.D.	N.D.	033	70
JuanFernandez	nz	-33.9	-81.8	1.0	084	±3	80	±20	081	62
SanFelix	nz	-26.4	-80.1	0.3	083	±8	N.D.	N.D.	080	61
Easter	nz	-26.4	-106.5	1.0	087	±3	95	±5	097	61
Galapagos	nz	-0.4	-91.6	1.0	096	±5	55	±8	086	48
Galapagos	co	-0.4	-91.6	0.5	045	±6	N.D.	N.D.	045	81
Louisville	pa	-53.6	-140.6	1.0	316	±5	67	±5	300	76
Foundation	pa	-37.7	-111.1	1.0	292	±3	80	±6	283	88
Macdonald	pa	-29.0	-140.3	1.0	289	±6	105	±10	295	88
Arago	pa	-23.4	-150.7	1.0	296	±4	120	±20	298	88
N.Austral	pa	-25.6	-143.3	B	293	±3	75	±15	296	88
Maria/S.Cook	pa	-22.2	-154.0	0.8	300	±4	N.D.	N.D.	299	88
Samoa	pa	-14.5	-169.1	0.8	285	±5	95	±20	301	88
Crough	pa	-26.9	-114.6	0.8	284	±2	N.D.	N.D.	285	89
Pitcairn	pa	-25.4	-129.3	1.0	293	±3	90	±15	291	89
Society	pa	-18.2	-148.4	0.8	295	±5	109	±10	297	89
Samoa	pa	-14.5	-168.2	0.8	285	±5	95	±20	301	88
Marquesas	pa	-10.5	-139.0	0.5	319	±8	93	±7	295	88
Caroline	pa	4.8	164.4	1.0	289	±4	135	±20	299	89
Hawaii	pa	19.0	-155.2	1.0	304	±3	92	±3	302	80
Guadalupe	pa	27.7	-114.5	0.8	292	±5	80	±10	294	54
Cobb	pa	46.0	-130.1	1.0	321	±5	43	±3	317	44
Bowie	pa	53.0	-134.8	0.8	306	±4	40	±20	327	42

Note: Entries are the hotspot and plate its track is on, its location (latitude, longitude), its weight 'w' (see Introduction in text for explanation of w), the observed azimuth (usually from most recent ~5-10 m.y.) with estimated error, the observed rate with estimated error, and the azimuth and rate predicted by our model.

* N.D. = not determined





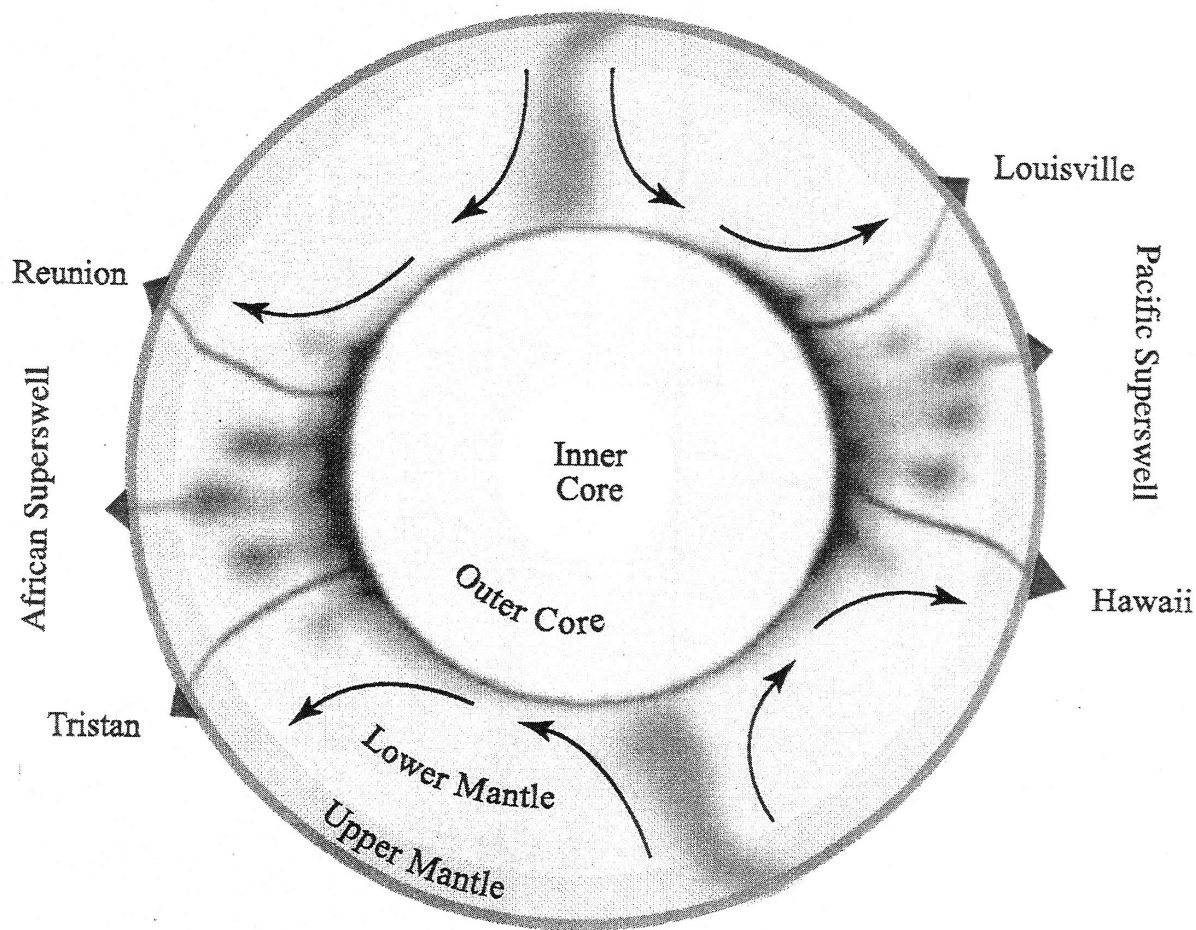


Figure 3